Lab on a Chip

Accepted Manuscript

This is an *Accepted Manuscript*, which has been through the Royal Society of Chemistry peer review process and has been accepted for publication.

Accepted Manuscripts are published online shortly after acceptance, before technical editing, formatting and proof reading. Using this free service, authors can make their results available to the community, in citable form, before we publish the edited article. We will replace this *Accepted Manuscript* with the edited and formatted *Advance Article* as soon as it is available.

You can find more information about *Accepted Manuscripts* in the **Information for Authors**.

Please note that technical editing may introduce minor changes to the text and/or graphics, which may alter content. The journal's standard **Terms & Conditions** and the **Ethical guidelines** still apply. In no event shall the Royal Society of Chemistry be held responsible for any errors or omissions in this *Accepted Manuscript* or any consequences arising from the use of any information it contains.

Liquid Phase Solvent Bonding of Plastic Microfluidic Devices Assisted by Retention Grooves

Alwin M.D. Wan[1], Amir Sadri[2], Edmond W.K. Young*[1,3]

[1] Department of Mechanical & Industrial Engineering, University of Toronto, Toronto, ON, Canada

[2] Bio-Rad Laboratories (Canada) Ltd., Mississauga, ON, Canada

[3] Institute of Biomaterials and Biomedical Engineering, University of Toronto, Toronto, ON, Canada

* Corresponding author:

Prof. Edmond W.K. Young

Department of Mechanical & Industrial Engineering

Institute of Biomaterials and Biomedical Engineering

University of Toronto, Toronto, ON, Canada

E-mail: eyoung@mie.utoronto.ca

Tel.: +1 (416) 978-1521

Fax: +1 (416) 978-7753

Abstract

We report a novel method for achieving consistent liquid phase solvent bonding of plastic microfluidic devices via the use of retention grooves at the bonding interface. The grooves are patterned during the regular microfabrication process, and can be placed at the periphery of a device, or surrounding microfluidic features with open ports, where they effectively mitigate solvent evaporation, and thus substantially reduce poor bond coverage. This method is broadly applicable to a variety of plastics and solvents, and produces devices with high bond quality (*i.e.*, coverage, strength, and microfeature fidelity) that are suitable for studies in physics, chemistry, and cell biology at the microscale.

Introduction

Microfluidics has emerged over the last two decades as a technology well suited for studying chemistry and physics at the microscale,[1] and with emerging potential to make significant contributions to cell biology research.[2–4] Microfluidic devices are also naturally amenable to high-throughput and integrated designs, paving the way toward lab-on-a-chip systems that are desirable for both academic and commercial applications.[5–8] In a typical laboratory setting, microfluidic devices are traditionally fabricated by soft lithography methods in poly(dimethylsiloxane) (PDMS), a silicone elastomer that is cheap, simple to use, and offers high quality feature replication below a spatial resolution of 10 microns.[9] However, while PDMS has enabled significant progress in microfluidics, it requires batch-to-batch mixing, degassing, and curing steps that are acceptable for low volume production, but are ultimately incompatible with high-volume manufacturing processes.[10,11] PDMS is also prone to bulk absorption of small hydrophobic molecules,[12] which is a significant problem for cell biology studies.[13,14] As such, there is a growing trend toward (a return to) plastic microfluidic devices, because of their much greater potential for translation to commercialization and mass manufacturing processes.

One of the major longstanding challenges facing plastic microfabrication, particularly in an academic setting, is achieving easy, high quality bonding of plastic parts. Current strategies employ thermal, adhesive, and solvent bonding techniques, but all suffer from significant challenges. Thermal bonding often distorts channel cross-sectional geometries[15–17] and increases the autofluorescence of plastic devices,[18] while adhesive bonding requires stencils and careful alignment to avoid clogging channels, and will leave the thickness of the adhesive layer exposed to sensitive fluidic components.[16] Solvent bonding in the vapor phase can be challenging, requiring vapor chambers and proper vacuum equipment, which increases the complexity and cost (both upfront capital, and maintenance) of the fabrication process.[19] Liquid phase solvent bonding, while more attractive due to its simplicity and low cost, often suffers from microfeature deformation and solvent evaporation effects that lead to inconsistent, non-uniform bonding near devices edges.

Despite these challenges, solvent bonding is a particularly promising avenue for sealing plastic microfluidic devices because of its inherent tunability that derives from the vast array of available solvents that can be selected or combined (particularly in the liquid-phase) for the specific plastic being used. Indeed, solvent bonding strategies have been reported for a wide variety of thermoplastics, including poly(methyl methacrylate) (PMMA),[20–24] polystyrene (PS),[25] polycarbonate (PC),[26] and cyclic

olefin polymer (COP).[25,27] Still, a widely-applicable strategy is needed to address common bond uniformity problems caused by solvent evaporation, particularly near free edges of devices or open ports. This can be difficult with many solvent/plastic systems, but is made especially challenging in microfluidic devices that often have a high density of microfeatures.

Here, we describe a unique way to achieve consistent liquid phase solvent bonding of microfluidic parts that yields uniform bond coverage, high-strength bonds, and preserves the geometry of microchannel features. The method utilizes a geometric retention groove that can be placed anywhere on the device *(i.e.*, surrounding various features, or at the edge of the device), and acts as a reservoir/sealant that mitigates local evaporation effects. This strategy effectively eliminates poorly-bonded regions within the area enclosed by the groove, and allows plastic devices to be consistently sealed with a high-strength, uniform bond. We demonstrate that this method is applicable to multiple combinations of plastics and solvents, and broadly enables solvent-bonded devices to be used for more complex studies of bonding *quality* (*i.e.*, uniformity, strength, and preservation of microfeature geometries), as well as for cell biology studies.

Materials and Methods

Plastic Device Fabrication

Devices were made from 1.5 mm thick sheets of poly(methyl methacrylate) (PMMA, McMaster Carr Supply Company, Elmhurst, IL, USA), 1.27 mm thick sheets of polystyrene (PS, Goodfellow Cambridge Ltd., Huntingdon, England), or 1.16 mm thick sheets of cyclic olefin polymer (COP, ZEONOR® 1020R, Zeon Corporation, Tokyo, Japan). All parts were fabricated with computer numerical control (CNC) milling using a Tormach PCNC 770 vertical milling machine (Tormach, Waunakee, WI). Microchannels and microfeatures (patterned into devices) were modelled with SolidWorks (Dassault Systemes, Velizy-Villacoublay, France). The CNC program was created with SprutCAM (SprutCAM, Naberezhnye Chelny, Russia). Devices were milled using 4 flute carbide endmills in sizes of 1/32" (794 μm), 0.02" (508 μm), and 0.01" (#89318919, # 37289873, and #37289857, MSC Industrial Supply Co., Melville, NY, USA), using procedures previously described.[28]

Solvent Bonding

PMMA and PS devices were bonded with acetone (ACS grade, Caledon Laboratories Ltd., Georgetown, ON, Canada) diluted in de-ionized (DI) water. PS devices were also bonded with acetonitrile (Bio Basic Canada Inc., Markham, ON, Canada) diluted in DI water. COP devices were bonded with

dichloromethane (Sigma-Aldrich Corporation, St. Louis, MO, USA) diluted in ethanol (Commercial Alcohols Inc., Toronto, ON, Canada). Prior to bonding, plastic devices were cleaned with laboratory soap and water, rinsed in DI water, and dried with dry nitrogen gas. The appropriate bonding solution was added in excess to one layer of the bonding stack by pipette, and the two layers were brought together to create a uniform film of solvent while avoiding air bubbles at the bonding interface. The bonding stack was placed on a pre-heated hotplate (20 minutes at 40°C for acetone/water, 10 minutes at 65°C for acetonitrile/water, and 10 minutes at 40°C for dichloromethane/ethanol), and pressure of 15 psi (103 kPa) was applied for the duration. After bonding, remaining liquid in open channels was removed with dry nitrogen gas, and the devices were left at room temperature overnight to allow any remaining solvent to evaporate.

Bond Coverage Measurements

Bonded devices were photographed with a camera (Canon Rebel T3), and the resulting photographs were analyzed for bond coverage in ImageJ (National Institutes of Health) by quantifying the area of the bonded and unbonded regions.

Bond Strength Measurements

Bond strength was evaluated using the wedge method reported by Maszara and coworkers.[29] Briefly, stainless steel shims of thicknesses 0.03" (762 μm) and 0.15" (381 μm) were each used to wedge apart bonded plastic layers. The delamination distance was measured from the leading edge of the shim (average of 10 measurements), and used to calculate the surface energy (representative of bond strength) of the bonding interface.

Microfeature Fidelity Measurements

The preservation of microfeature geometry (*i.e.*, fidelity) was evaluated by imaging cross-sections of bonded microchannels. Cross-sections were obtained by cutting devices with a CNC milling machine. The cross-sections were imaged on an EVOS FL Auto Cell Imaging System inverted microscope (Life Technologies, Carlsbad, CA, USA). The resulting images were analyzed in ImageJ (National Institutes of Health) to quantify the area and perimeter of the channel cross-sections, before and after bonding.

Cell Culture

Cell culture experiments were performed in PMMA devices, each with three straight channels of dimensions 1.5 mm wide × 0.5 mm deep × 10 mm long. Devices were disinfected with 70% ethanol in

water for 20 minutes, and subsequently rinsed with sterile PBS (Life Technologies) 3 times. After this, human umbilical vein endothelial cells (HUVECs) were seeded at a density of 4000 cells/µL in EBM Basal Medium containing SingleQuot supplements (Lonza, Allendale, NJ, USA). The devices were placed in an incubator (37°C, 5% CO_2) and allowed to culture for 24 hours. After 24 hours of culture time, the HUVECs within the devices were chemically fixed, blocked, and immunostained with monoclonal mouse anti-human PECAM-1 antibody (MCA1738, Cedarlane Laboratories, Burlington, ON, Canada), goat anti-mouse AlexaFluor 488 secondary antibody (A-11001, Life Technologies), and Hoechst 33342 nuclear stain (H1399, Life Technologies). Images of the cultures were obtained on an EVOS FL Auto Cell Imaging System inverted fluorescence microscope (Life Technologies).

Results

Solvent Bonding Process

The general liquid phase solvent bonding process used here is shown in Figure 1. First, the solvent solution is added to one of the clean bonding surfaces (by pipette, eyedropper, or other dispensing tool). The surfaces are then brought into contact, ensuring that the presence of air bubbles is minimized, as trapped air bubbles can cause localized regions of unbonded plastic. It should be noted that the solvent solution typically fills (or partially fills) the microfeatures of the device during this step. As such, the surfaces of microchannels in solvent-bonded devices will be exposed to the solvent, unless a specific strategy is employed to avoid this. After the bonding surfaces are brought together, both elevated temperature and pressure are typically applied to the bonding stack to activate or accelerate the solvent-assisted softening of the bonding interface, and to facilitate bonding of the two layers via interdiffusion of polymer chains across the interface. After sufficient bonding time, the bonded device is removed from heat and pressure, and any remaining liquid in the device can be removed through open ports via pressurized gas, vacuum, or other methods.

Solvent Retention Groove

One common challenge associated with solvent bonding is bond coverage, particularly near device edges that are open to air. Evaporation at the free edges of the chip – caused by the inherent volatility of the solvent (particularly at elevated temperatures), as well as the limited volume of solvent that is present between the bonding layers – can rapidly cause the solvent line to recede from the boundary of the chip before bonding occurs. This leads to regions of unbonded plastic, which can negatively impact device performance (*i.e.*, resulting in "leaky" devices), and lower the total bond strength of the finished device. To address this challenge, we introduced a simple groove to one of the bonding layers during

the fabrication process (Figure 2A). This groove retains additional solvent near the free edge of the chip, thus mitigating the effects of evaporation during the bonding process. As shown in Figure 2B, we observed that the addition of this groove significantly improved bond coverage, and unbonded regions were restricted to the outside of the groove (*i.e.*, between the groove and the free edge of the chip).

Importantly, the geometry of the solvent retention groove is flexible. It can be constructed at the periphery of the chip as described above to assist with bond coverage at the edges, or it can alternatively (or additionally) be constructed around individual features, such as channels with open ports. When constructed around features, we observed these grooves to significantly improve bond coverage at these critical locations, ensuring that features were properly sealed and that the device functioned as designed, without any leakage.

These bond coverage effects can be quantified by measuring, in the presence or absence of grooves, the total unbonded area at the periphery of the device and surrounding each feature. The area can be normalized to the perimeter of the feature in question, yielding an effective "width" of the unbonded region that surrounds the feature. We observed that grooves in both locations (peripheral and feature) effectively and independently reduced the amount of unbonded area in their respective locations (Figure 2C). Thus, this simple technique significantly improves the uniformity of bond coverage, which is an important characteristic of a high quality bond, and is a common challenge for liquid phase solvent bonding methods. From a practical standpoint, it also enables consistent fabrication of functional (*i.e.*, properly sealed) devices with arbitrarily complex designs. For these reasons, we chose to use devices with grooves for all of our subsequent studies.

Bond Strength

Liquid solvents are convenient to use, but can potentially be too aggressive for certain plastics if used at high concentrations; however, they can be diluted to tune their aggressiveness. We varied the concentration of acetone in a solution with water to bond PMMA layers, and saw softening of the polymer with excessively high concentrations, but weak bonds (with poor bond coverage) at low concentrations. To this end, we sought to quantify both bond strength and microfeature fidelity (*i.e.*, the preservation of microchannel cross-sectional geometries) as functions of solvent concentration. To measure bond strength, we used a wedge method reported by Maszara and coworkers,[29] wherein a shim of known thickness is wedged between two bonded layers, and the delamination distance is measured

from the leading edge of the shim. From this, the surface energy γ (representative of the bond strength) is calculated by the equation

$$\gamma = \frac{3}{8}\frac{Et^3 y^2}{L^4} \tag{1}$$

where E is the elastic modulus of the plastic, t is the thickness of each plastic layer, y is half the shim thickness, and L is the delamination distance (Figure 3A).

Using this method, we measured the bond strength between PMMA layers that were bonded with varying concentrations of acetone (diluted in deionized (DI) water). We selected acetone as the solvent for PMMA based on the similarity of their respective Hildebrand solubility parameters ($\delta \sim 20.1$ MPa$^{1/2}$ for PMMA and $\delta \sim 20.4$ MPa$^{1/2}$ for acetone),[16] which suggested a high degree of mutual solubility. Indeed, pure acetone dissolves PMMA very aggressively, as Shah and coworkers reported that exposure time to acetone had to be limited to less than 3 s to prevent microchannel deformation.[30] Thus, we diluted acetone with DI water to tune its aggressiveness (Figures 3B–C), and subsequently measured the effect of acetone concentration on bond strength. As shown in Figure 3D, the bond strength increased with acetone concentration as expected, with a slight plateauing of the curve toward pure acetone.

We next extended this to bonding different plastics with different solvents, using reported solubility parameters[16] to guide our solvent choices. We tested: polystyrene (PS, $\delta \sim 18.7$) with acetone (Figure 3E), cyclic olefin polymer (COP, $\delta \sim 17.7$) with dichloromethane ($\delta \sim 19.8$) (Figure 3F), and PS with acetonitrile ($\delta \sim 25.1$) (Figure 3G). Acetone and acetonitrile were diluted with DI water, whereas dicholoromethane was diluted with ethanol due to its immiscibility with water (we note that ethanol ($\delta \sim 26.0$) does not react with COP). In all cases, bond strength followed the same expected trend, increasing with solvent concentration.

Microfeature Fidelity

While bond strength increases with solvent concentration due to the aggressiveness of the solvent, so does deformation of microscale features such as channels (Figure 3B-C), which is detrimental to the precise operation of a microfluidic device. Thus, selecting an optimal solvent concentration to seal a practical microfluidic device must involve considerations of not only bond strength, but also the fidelity of microfeatures after bonding. To this end, we sought to quantify the fidelity of microchannels after solvent bonding at varying solvent concentrations. We focused on PMMA (bonded with an acetone solution), and studied cross-sections of bonded channels to assess two measures of channel fidelity: (1)

the change (decrease) in cross-sectional area, and (2) the rounding of the cross-section due to polymer softening, measured by circularity $C = 4\pi A/P^2$, where A is the cross-sectional area, and P is the cross-sectional perimeter (Figure 4A). Plotting these parameters provided a "map" of channel fidelity as a function of solvent concentration (Figure 4B). As a reference, for square cross-sections, $C = \pi/4 = 0.79$, while for circular cross-sections, $C = 1$. Using these data in conjunction with bond strength measurements (Figure 3), we suggest that both 75% and 80% acetone concentrations in DI water are optimal PMMA bonding concentrations. While 80% acetone has more than 2.5x the bond strength compared to 75% acetone (34.4 J/m^2 vs. 13.6 J/m^2), 75% acetone has slightly lower area reduction and circularity (*i.e.*, higher quality). Furthermore, the bond strength from applying 75% acetone on PMMA was found to already surpass reported bond strengths from thermal bonding strategies using high pressure and long bonding times (4000 lbf and 60 min on PS leads to ~6.0 J/m^2).[17] We therefore chose to use 75% acetone in the subsequent experiments described below.

Cell Culture Applications

Thermoplastics are particularly attractive materials for use in biological applications due to their ease of processing, high optical transparency, inertness to small hydrophobic biomolecules, and widespread acceptance (of polystyrene) in the biological sciences. Thus, we sought to investigate the utility of solvent-bonded thermoplastic devices for cell-culture applications, and specifically, whether the surfaces exposed to solvent would adversely affect cell behavior. We fabricated PMMA devices with straight microchannels, bonded at the optimal 75% acetone concentration, and cultured human umbilical vein endothelial cells (HUVECs) in the channels. After 24 hours of culture, we stained the cells for platelet endothelial cell adhesion molecule (PECAM-1), a signature cell-surface marker of endothelial cells. The HUVECs formed a confluent monolayer, as highlighted very clearly by positive PECAM-1 staining at the cell-to-cell junctions (Figure 5). This indicates that they were able to adhere, proliferate, and perform regular cell functions (as evidenced by their display of the typical cobblestone morphology observed in endothelial cell monolayers). This suggests that the cells were unaffected by the surfaces of the microchannels that were exposed to solvent, although further studies are required to investigate more complex cell functions.

As further demonstration of the quality of bonds achieved by our method, we also investigated whether bonding was affected by the warm, humid environment of a cell culture incubator by placing PMMA devices (bonded with 75% acetone) in an incubator for 48 hours. When we subsequently measured bond strength, we found no difference when compared to non-incubated devices (Figure 6). Further, we

also found no difference between incubated devices with grooves and without grooves. This was expected, since while the grooves improve bond coverage and uniformity, they do not alter bond strength (which is solely a function of bonding parameters, such as solvent concentration). In practice, we have used such solvent-bonded devices for cell culture experiments lasting one week, and did not observe any change in the bonding over that time. These results demonstrate that solvent-bonded devices remain durable during extended culture periods, and are suitable for long-term cell biology studies.

Discussion

Our results indicate that adding grooves to plastic microfluidic devices significantly improves the uniformity of bond coverage achieved with liquid phase solvent bonding for a variety of plastics and solvents. This enables the practitioner to consistently fabricate properly sealed devices, while taking advantage of the benefits solvent bonding has over other bonding methods (such as simplicity and high bond strength[16]). One notable drawback of this method is that the grooves take up potentially valuable real estate on the chip. For example, in this work, we used grooves with cross-sections of 500 μm × 500 μm, and placed them 300 μm away from the edge of the device or feature. Thus, a groove used 800 μm of additional space to surround a feature. While this was not an issue for our devices, which did not require a high density of microchannels, such (relatively large) dimensions could clearly pose a problem for designs that require very close spacing between microfeatures. In such cases, however, this effect can be mitigated to some extent by reducing the groove width and offset distance from features.

We chose to use such "large" grooves for two reasons: (i) because our microfeature density did not necessitate narrower grooves, and (ii) because of time considerations during our micromilling fabrication process – narrower grooves would require smaller endmills for machining, which must be operated at correspondingly slower speeds,[28] thus slowing down the fabrication process. It should be noted, however, that we utilized micromilling for its rapid prototyping capabilities, and that any higher-volume manufacturing process would use a technique such as hot-embossing or injection molding. With such techniques, there is no time penalty associated with using narrower grooves, and they could be placed much closer to the edge of features as well. Further study is required to determine the minimum groove size and offset spacing that would still enable uniform bond coverage, but we have had success using groove sizes below 250 μm × 250 μm, and offset spacings below 50 μm. The aspect ratio of the groove can also be altered, with higher aspect ratios (taller and narrower) potentially offering the same

benefits regarding bonding, while using less space on a device. Nonetheless, grooves will always occupy some space on the device, and thus may not be amenable for use with all designs.

As described above, we chose our solvents for each plastic based on published solubility parameters, and with a preference for less harmful or toxic chemicals where possible (*e.g.*, preferring acetone ($\delta = 20.4$ MPa$^{1/2}$) over dichloromethane ($\delta = 19.8$ MPa$^{1/2}$) for bonding PMMA ($\delta = 20.1$ MPa$^{1/2}$) and PS ($\delta = 18.7$ MPa$^{1/2}$). We used dichloromethane to bond COP because acetone does not react with COP at all.

Regarding our choice of diluents, a note on dimethyl sulfoxide (DMSO) is warranted. DMSO is well known to be miscible with a wide variety of chemicals, including both solvents used in this work (*i.e.*, acetone and dichloromethane). Given its Hildebrand solubility parameter ($\delta = 26.7$ MPa$^{1/2}$),[16] it might seem like an appropriate candidate to use for diluting the solvents used in this work. However, DMSO has two major drawbacks: (i) it is toxic to cells even at low concentrations,[31] and (ii) it leaches plastic additives out of the bulk and into solution that can have adverse effects on biological functions.[32] Thus, we chose to avoid DMSO, and instead used DI water and ethanol as diluents to tune the aggressiveness of our solvents.

Conclusions

Liquid phase solvent bonding is an attractive method for sealing plastic microfluidic devices because of its simplicity, low cost, and high resulting bond strength, but is not commonly used due to typically cited issues with over-aggressiveness of solvents, or evaporation near free edges that leads to poor bond uniformity. We have demonstrated that adding simple grooves to plastic microfluidic devices mitigates evaporation effects, and thus enables the use of liquid phase solvent bonding to achieve consistent, uniform, high-strength bonds for a variety of plastics and solvents. Further, this enabled us to freely tune the aggressiveness of our solvents via dilution without having to worry about poor bond coverage for weaker solvent solutions, allowing us to find optimal solvent concentrations that balanced high bond strength with high fidelity of microfeature geometries. Together, our findings suggest that liquid phase solvent bonding assisted by grooves represents a broadly applicable method for fabricating plastic microfluidic devices with high efficiency, with few failed devices due to leaky bonding. Devices made with this method were well suited for studies of bond quality (*i.e.*, bond coverage, bond strength, and microfeature fidelity), as well as for applications in long-term cell biology studies. While consideration must be given to the space that a groove might occupy on a device, this technique should be applicable

to a wide variety of designs, for low- to high-volume manufacturing methods, and may pave the way toward greater adoption of plastic microfluidics for both laboratory and commercial applications.

Acknowledgements

References

1   D. J. Beebe, G. A. Mensing and G. M. Walker, *Annu. Rev. Biomed. Eng.*, 2002, **4**, 261–286.

2   C. Situma, M. Hashimoto and S. a. Soper, *Biomol. Eng.*, 2006, **23**, 213–231.

3   A. L. Paguirigan and D. J. Beebe, *BioEssays*, 2008, **30**, 811–821.

4   E. W. K. Young and D. J. Beebe, *Chem. Soc. Rev.*, 2010, **39**, 1036–1048.

5   D. Erickson and D. Li, *Anal. Chim. Acta*, 2004, **507**, 11–26.

6   C. H. Ahn, J.-W. Choi, G. Beaucage, J. H. Nevin, J.-B. Lee, A. Puntambekar and J. Y. Lee, *Proc. IEEE*, 2004, **92**, 154–173.

7   D. S. Kim, S. H. Lee, C. H. Ahn, J. Y. Lee and T. H. Kwon, *Lab Chip*, 2006, **6**, 794–802.

8   S. Haeberle and R. Zengerle, *Lab Chip*, 2007, **7**, 1094–1110.

9   D. C. Duffy, J. C. McDonald, O. J. A. Schueller and G. M. Whitesides, *Anal. Chem.*, 1998, **70**, 4974–4984.

10   E. Berthier, E. W. K. Young and D. Beebe, *Lab Chip*, 2012, **12**, 1224–37.

11   E. K. Sackmann, A. L. Fulton and D. J. Beebe, *Nature*, 2014, **507**, 181–9.

12   M. W. Toepke and D. J. Beebe, *Lab Chip*, 2006, **6**, 1484–1486.

13   K. J. Regehr, M. Domenech, J. T. Koepsel, K. C. Carver, S. J. Ellison-Zelski, W. L. Murphy, L. a Schuler, E. T. Alarid and D. J. Beebe, *Lab Chip*, 2009, **9**, 2132–2139.

14   X. Su, E. W. K. Young, H. A. S. Underkofler, T. J. Kamp, C. T. January and D. J. Beebe, *J. Biomol. Screen. Off. J. Soc. Biomol. Screen.*, 2011, **16**, 101–111.

15   T. I. Wallow, A. M. Morales, B. A. Simmons, M. C. Hunter, K. L. Krafcik, L. A. Domeier, S. M. Sickafoose, K. D. Patel and A. Gardea, *Lab Chip*, 2007, **7**, 1825–1831.

16   C. W. Tsao and D. L. DeVoe, *Microfluid. Nanofluidics*, 2009, **6**, 1–16.

17   E. W. K. Young, E. Berthier, D. J. Guckenberger, E. Sackmann, C. Lamers, I. Meyvantsson, A. Huttenlocher and D. J. Beebe, *Anal. Chem.*, 2011, **83**, 1408–1417.

18   E. W. K. Young, E. Berthier and D. J. Beebe, *Anal. Chem.*, 2013, **85**, 44–49.

19   C. Eberspacher, C. Fredric, K. Pauls and J. Serra, *Thin Solid Films*, 2001, **387**, 18–22.

20   L. J. Kricka, P. Fortina, N. J. Panaro, P. Wilding, G. Alonso-Amigo and H. Becker, *Lab Chip*, 2002, **2**, 1–4.

21   H. Klank, J. P. Kutter and O. Geschke, *Lab Chip*, 2002, **2**, 242–6.

22   R. Truckenmüller, P. Henzi, D. Herrmann, V. Saile and W. K. Schomburg, *Microsyst. Technol.*, 2004, **10**, 372–374.

23   L. Brown, T. Koerner, J. H. Horton and R. D. Oleschuk, *Lab Chip*, 2006, **6**, 66–73.

24   X. Sun, B. a. Peeni, W. Yang, H. a. Becerril and A. T. Woolley, *J. Chromatogr. A*, 2007, **1162**, 162–166.

25   A. Bhattacharyya and C. M. Klapperich, *Lab Chip*, 2007, **7**, 876–82.

26   D. Ogończyk, J. Wegrzyn, P. Jankowski, B. Dabrowski and P. Garstecki, *Lab Chip*, 2010, **10**, 1324–7.

27   C. W. Tsao, L. Hromada, J. Liu, P. Kumar and D. L. DeVoe, *Lab Chip*, 2007, **7**, 499–505.

28   D. J. Guckenberger, T. de Groot, A. M. D. Wan, D. Beebe and E. Young, *Lab Chip*, 2015, **15**, 2364–2378.

29   W. P. Maszara, G. Goetz, A. Caviglia and J. B. McKitterick, *J. Appl. Phys.*, 1988, **64**, 4943–4950.

30   J. J. Shah, J. Geist, L. E. Locascio, M. Gaitan, M. V. Rao and W. N. Vreeland, *Anal. Chem.*, 2006, **78**, 3348–3353.

31   W. Qi, D. Ding and R. J. Salvi, *Hear. Res.*, 2008, **236**, 52–60.

32   G. R. McDonald, A. L. Hudson, S. M. J. Dunn, H. You, G. B. Baker, R. M. Whittal, J. W. Martin, A. Jha, D. E. Edmondson and A. Holt, *Science*, 2008, **322**, 917.
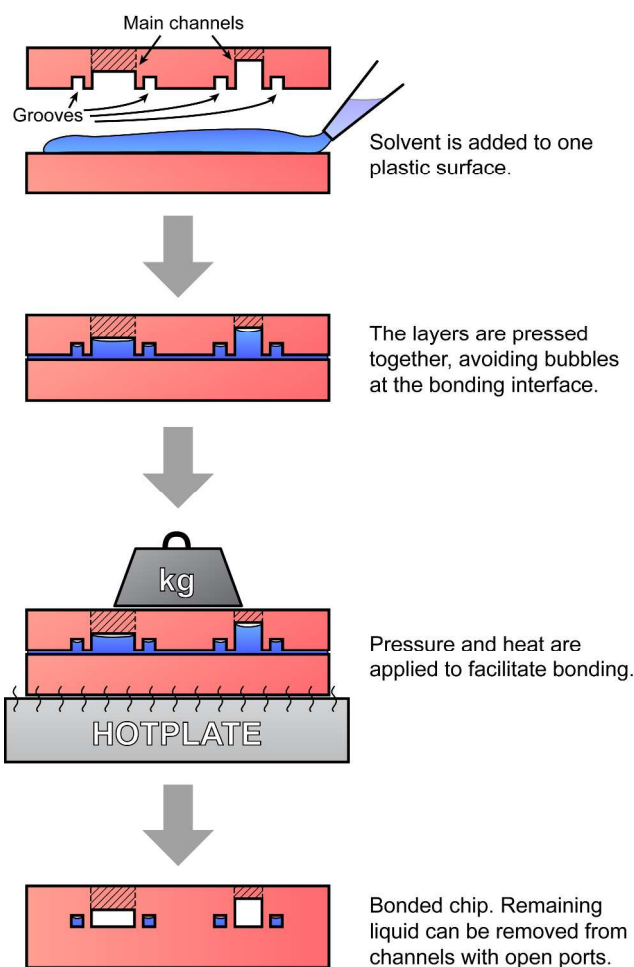
Figure 1 – Schematic illustrating a typical liquid phase solvent bonding process used to seal a plastic microfluidic chip. Solvent is first added between plastic layers, which are then pressed together. Excess solvent will often partially (or fully) fill features such as channels and grooves. Pressure and heat are applied to facilitate the bonding process. After bonding is complete, any remaining liquid in the channels is removed via the open ports of the bonded chip (shown schematically as hatched regions), while liquid in enclosed grooves remains.
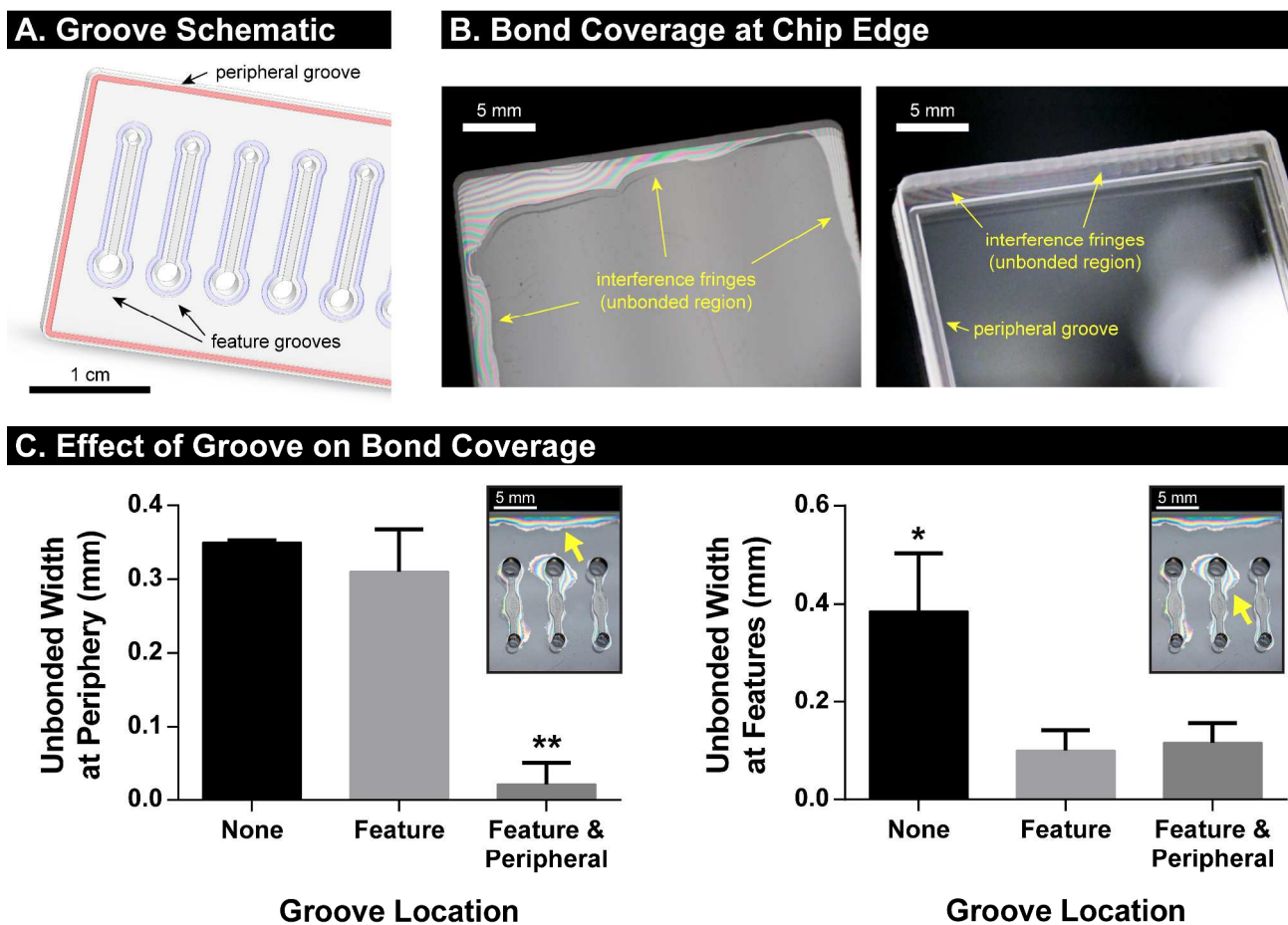
Figure 2 – (A) A schematic shows a generic device layer with straight channels and ports as features. Solvent retention grooves are easily added to the design, and with adaptable geometry. Grooves can be placed near the periphery of the device (highlighted in red), or surrounding important features (highlighted in blue). **(B)** Photographs of solvent-bonded PMMA chips demonstrate the effect of the groove. At left, a chip with no groove exhibits typically poor bond coverage near the edges, visible due to colored interference fringes from the unbonded region. At right, a chip with a peripheral groove exhibits substantially improved bond coverage, with unbonded regions restricted to the outside of the groove. **(C)** The effect of the groove is quantified by measuring the average width of the unbonded region (calculated as the measured unbonded area divided by the perimeter of the feature). At left, the unbonded width at the periphery of the chip is substantially decreased with the addition of a peripheral groove, and unaffected by the presence of feature grooves. At right, the unbonded width surrounding individual features is substantially decreased with the addition of feature grooves, and is unaffected by the presence of a peripheral groove. The inset photographs indicate example locations of the measured unbonded area for each graph. Bars show standard deviations for at least $n = 3$. * indicates $p < 0.05$ and ** indicates $p < 0.01$ (Tukey-Kramer Post-Hoc test).
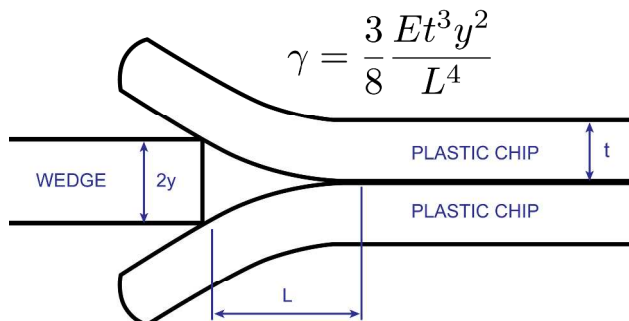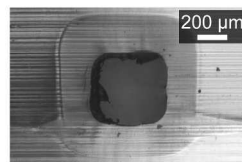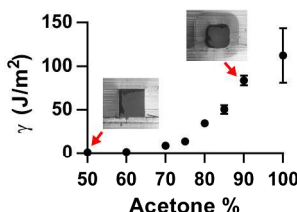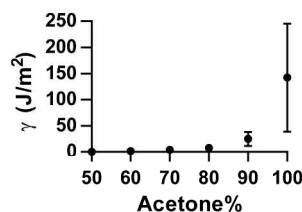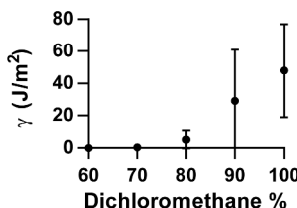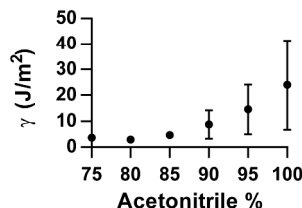
Figure 3 – (A) A schematic illustrates the wedge method used to measure bond strength (represented by surface energy γ). A shim of thickness *2y* is inserted between two bonded layers of thickness *t,* made of plastic with elastic modulus *E*. The delamination length *L* is measured, and used to calculate γ with the given equation. **(B) – (C)** Brightfield micrographs show the cross-sections of square 500 μm × 500 μm microchannels, bonded with 50% and 90% acetone solutions, respectively. The more aggressive (90%) solvent solution results in a microchannel that is visibly smaller and more rounded. These images are replicated in (D) with their corresponding bond strength data. **(D) – (G)** Bond strength was measured as shown in (A), as a function of varying solvent concentration, for: (D) PMMA bonded with acetone, (E) PS bonded with acetone, (F) COP bonded with dichloromethane, and (G) PS bonded with acetonitrile. Acetone and acetonitrile were diluted with DI water, while dichloromethane was diluted with ethanol due to immiscibility with water (ethanol does not react with COP). For all conditions, bars show standard deviations for at least *n* = 3.
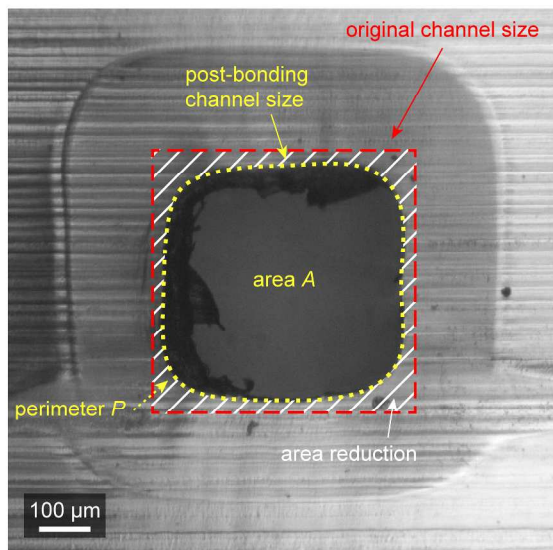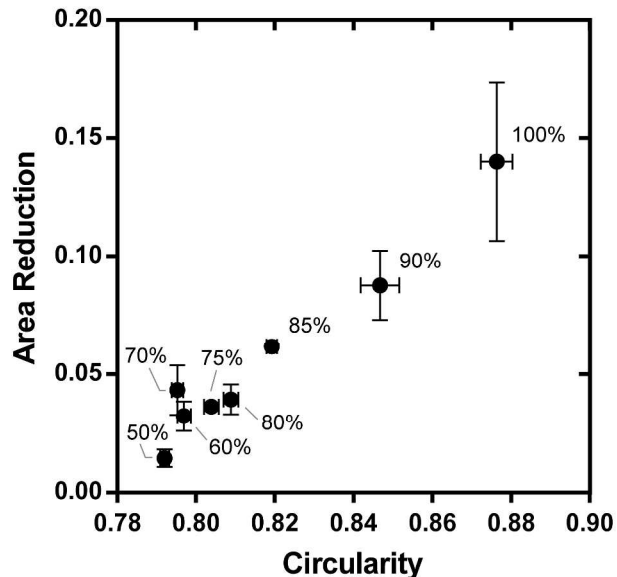
Figure 4 – **(A)** A brightfield micrograph shows the cross-section of a PMMA channel (outlined with a dotted yellow line), after being bonded with a 90% acetone solution. The red dashed outline shows the size of the original (unbonded) 500 µm × 500 µm channel. **(B)** Fidelity of bonded channels was assessed in terms of: fractional change (reduction) in cross-sectional area after bonding, and cross-sectional circularity ($C = 4\pi A/P^2$), as a function of varying acetone concentration. As a reference, for square cross-sections, $C = \pi/4 = 0.79$, while for circular cross-sections, $C = 1$. The region toward the bottom-left is preferred and represents high fidelity (minimal area change and rounding of channel), whereas the region toward the top-right represents low fidelity (significant area change and rounding of channel). For all conditions, bars show standard deviations for at least $n = 3$.
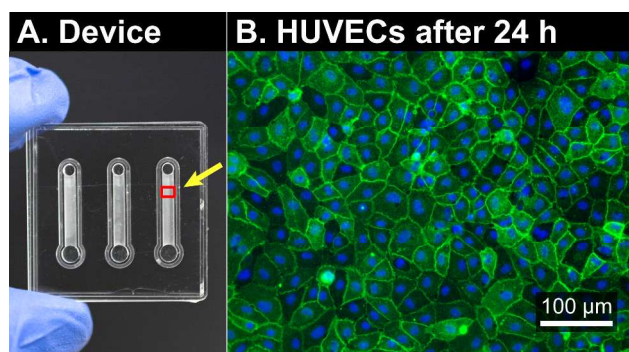
Figure 5 – **(A)** A photograph showing a typical PMMA device with straight microchannels that was used to culture HUVECs. The devices were bonded with 75% acetone in DI water. **(B)** After 24 hours of culture, cells were chemically fixed, and stained for PECAM-1 (green) and nuclei (blue, Hoechst). The positive PECAM-1 staining, as well as the clear formation of a cobblestone monolayer, indicate that the HUVECs behaved as expected, and did not appear to be adversely affected by the plastic surfaces subjected to the solvent bonding process.
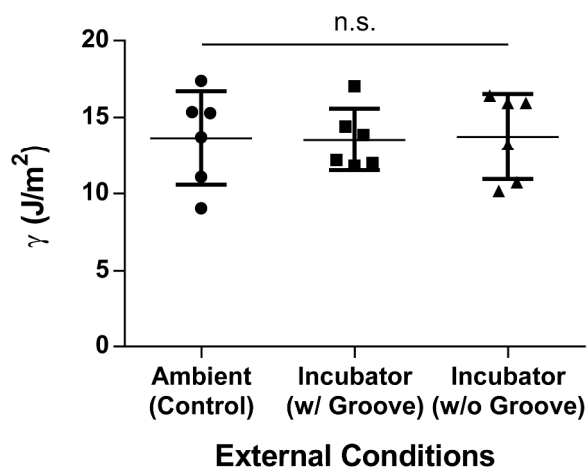
Figure 6 – Bond strength (represented by surface energy γ) as measured by the wedge method, for PMMA devices that were stored for 48 hours at ambient (room) temperature and humidity (Control), or at elevated temperature (37°C) and humidity (100%) (*i.e.*, cell culture incubator conditions). All devices were bonded with the optimal 75% acetone solution, and devices stored in the incubator had either a peripheral groove, or no groove. In all cases, bond strength was the same. n.s. = no statistical difference.